# Source of AEs from IG-SCC of Face Centered Cubic Metals under Static or Dynamic Straining

Mikio Takemoto, Shuichi Ueno and Motoaki Nakamura
Kanmeta Engineering Co. Ltd,Nakanocho-Higashi,2-3-54, Tondabayashi, Osaka, 584-0022,Japan

**ABSTRACT**: Stress Corrosion Cracking (SCC) of Face Centered Cubic (FCC) metals such as sensitized Type -304 and -316 by tetra-thionic acids and 70Cu/30Zn brass by ammonia vapor are intergranular (IG) type. These SCCs produce no AE when static SCC test are done. However, when we employ a dynamic strain test such as strain increasing test, these SCCs produce AEs even if it is done in non-corrosive environment. Detail SEM observation of fracture surfaces suggests that the coincident twin/austenitic grain boundaries with low energy are broken mechanically by dynamic loading and produce AEs. This paper discusses relationship between the extrusions observed on the fracture surface and the coincident grain boundaries.

## 1 INTRODUCTION

Among the environmental assisted cracking, active path corrosion type stress corrosion cracking (APC-SCC) has been recognized to emit no AE[1][2][3]. Typical example of the APC-SCC is the chloride SCC of austenitic stainless steel and transgranular (TG) type cracking. Though a very few AE can often be monitored for a limited material -environment combination, these AEs are mostly from the cracking of the corrosion products in the SCC, and not the primary AE from the initiation and propagation of the SCC[4]. Independently on the crack types (TG or IG) , we never monitor the primary AEs as long as a static loading such as bent beam testing is utilized. Authors have, however, reported that the primary AEs can be monitored for the IG-SCC when a continuously increasing load such as CERT (constant extension rate testing) is employed. We do not necessary need the CERT for producing the primary AEs, rather the dynamic loading or stepwise or continuously increasing loading is enough. The authors have called these AE behaviors as the unique AE so far[5]. However we do not understand the source mechanism of the unique AE. Once Takemoto estimated that the AE are possibly produced by fracture of the "weakly bond intact portion" of the grain boundary for the IG-SCC of Type-304 steel[6]. He also reported that the "extrusion like projections" were often observed on the grain boundary. However we could not understand what is the extrusion and how the extrusion is produced by what mechanism.
This research aims to study the possible source mechanism of AEs which are monitored during the crack opening operation or dynamic loading of the member which previously suffered IG-SCC. We estimate the source mechanism of the AEs, based on the detail fractographic observation of the fresh fracture surface produced by the crack opening operation. We insist an importance of the twin/austenite low energy grain boundary or coincident grain boundary in producing AEs..

## EXPERIMENTAL

Two kinds of material/environment combinations, sensitized stainless steels: Type-304 and -316 strips (2~3mmT-20mmW-67mmL) in 1 mass% tetra-thionic acid solution ( pH=2 ) and as-received 70Cu-30Zn brass in ammonia vapor (mainly 8% vapor) are tested. SCCs were induced into these strips by three point bending (static loading) SCC test and then washed by an ultrasonic washer three times and dried by hot air at being loaded. Some strips were kept in a desiccator for more drying. These strips were then submitted to a crack opening operation in air mainly, but for special aims in dry nitrogen gas or the corrodant. The crack opening aims to open the closed cracks in front of open SCC, and was done by turning the central bolt of the bending device continuously. Thus the crack opening operation is dynamic or continuously load increasing type. AEs were monitored by the two resonant type small sensors (PAC PICO) attached on the convex surface of the bent strip, and amplified to 40dB by a preamplifier and stored in a personal computer as digital data. Signals were analyzed by a home-made ADAS system.

## 3 RESULTS AND CONSIDERATION

### *3.1 IG-SCC of sensitized Type-304Steel by tetra-thionic acid*

Using the procedure of Figure 1, we first studied how long the closed IG-SCC was. Here the closed SCC implies the gain boundaries which could not be recognized as the crack by transverse microscopic observation.

The SCC strip tested by three point bending at arc height(AH) of 0.6 mm was longitudinally cut into two pieces by wire discharge cutting. One strip(A) was submitted to the AE monitoring and transverse microscopic observation after the crack open operation, and another one(B) to microscopic observation without opening operation. Figure 2 compares the crack depth before and after the opening operation. It can be seen that closed crack length reaches to 0.42 mm in this case. Figure 3 compares the SEMs of open (the left) and closed crack. The surface of newly produced by the opening operation are free from thick film (tarnish film of FeS) while that of the open crack possesses thick film. We can not obtain any fractographic information from the open crack but can from clear fracture surface. Figure 4 shows AE behavior during the static SCC test and the crack opening operation. We monitored no AE during 22 hours of the static SCC test (three point bending test), but 37 signals during the opening operation in air. Above the arc height (AH) of 1.3 mm, we again observed no AE since the attacked grains (closed crack) was completely opened. Figure 5

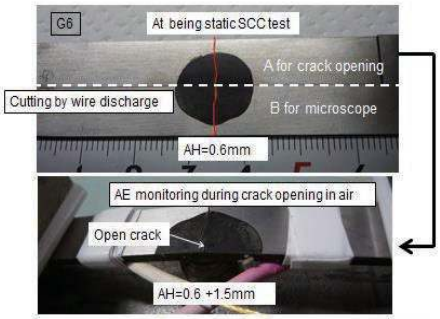


Figure 1: specimen with IG-SCC by static three point bending (the upper) and AE monitoring method during the crack opening of the longitudinally cut specimen

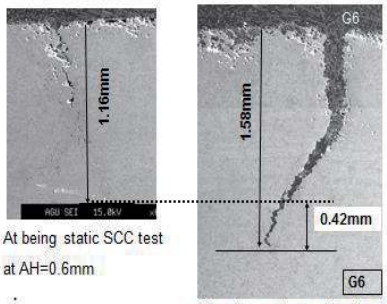


Figure 2: transverse IG-SCC of sensitized (650℃x 90min) type-304 steel by 1% tetra-thionic acid (pH=2).

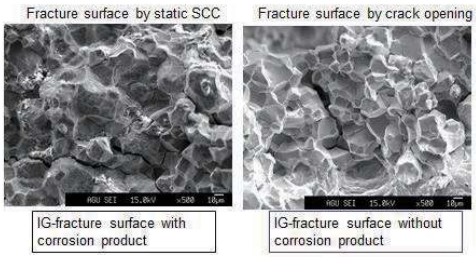


Figure 3: SEM of fracture surfaces by the static SCC test (the left) and by the crack opening operation of the sensitized type-304 (650℃x90min) by 1% tetra-thionic acid (pH=2)

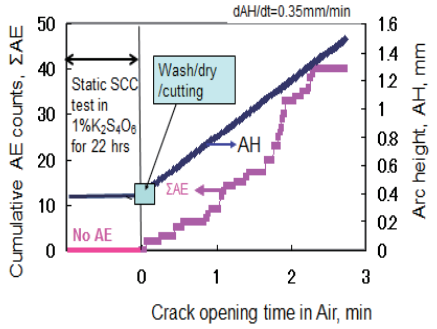


Figure 4:Acoustic emission during the static SCC test and the crack opening operation of the type-304 steel strip

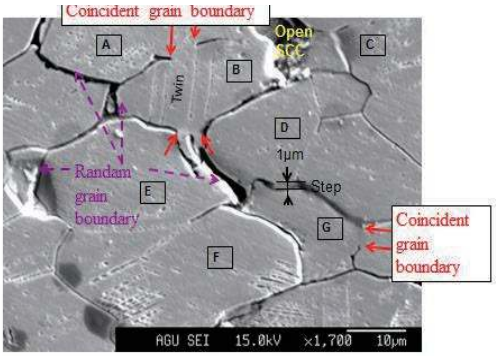


Figure 5:SEM of the free surface of type-304 strip with IG-SCC after the crack opening operation in air

shows SEM of transverse surface after the opening operation (Specimen A of Fig.1). There observed both the deeply attacked grain boundary and not attacked boundary. The former grain boundary corresponds to the random grain boundary or high energy boundary. Contrary, non-attacked portion corresponds to the coincident grain boundary with low energy. It is reported that the coincident boundaries are often produced at twin/austenite grain boundary[7][8]. This boundary seems to correspond to the "intact boundary" in authors previous report [6]. We also observe grain rotation and steps between the grains. We monitored fluctuation of the strain using the strain gage mounted over the cracks, and found rapid fluctuation with strain amplitude of $100x10^{-6}$ frequently. This means that the grains in the closed crack region actively move and rotate and produce AEs when the intact portion or the coincident grain boundary was mechanically fracture. Figures 6,7and 8 are SEMs of the fracture surface produced by the opening operation.

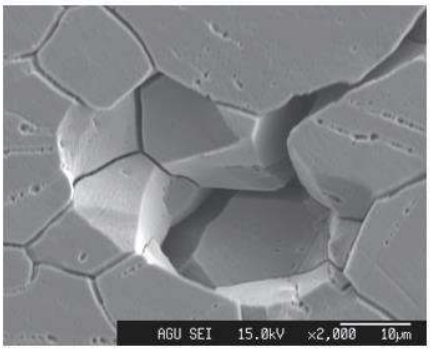


Figure 6:Falling-off of grains in sensitized type-304 steel by the corrosion of random grain boundaries

As the Figure 6 is the fractography of the grain–falling from the random grain boundaries, we do not observe any extrusion. Contrary, Figure 7 of the new fracture surface produced by the crack opening operation, we observe many extrusions. These extrusions are considered to be produced by tearing-off of the twins from the austenitic grain boundaries. We also observe the open sub-cracks or the open crack to the fracture surface, around the grains with the extrusions. This is because the grain colony with many extrusions are mechanically separated from the neighboring grains. Figure 8 shows small size cracks and in-tact portion (size in few micrometers) on the grain boundary. We observe many extrusions on the grain a.

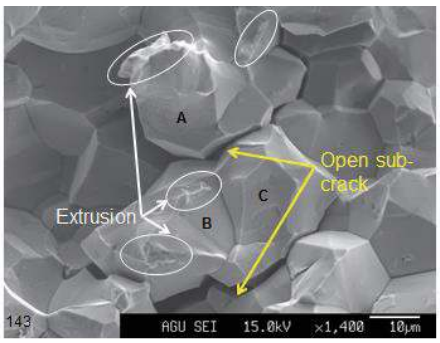


Figure 7:SEM of the fracture surface produced by the crack opening operation in air of the type-304 strip previously SCC tested in 1% tetra-thionic acid

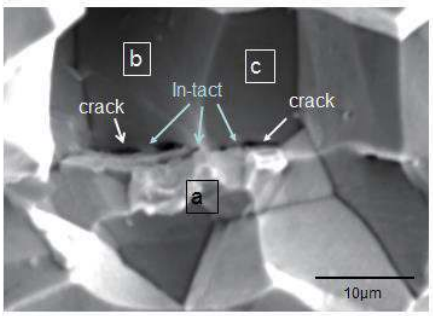


Figure 8:SEM of the fracture surface produced by crack opening operation of the type-304 strip previously SCC tested in 1% tetra-thionic acid.

We next studied the fluctuation of corrosion potential during the step-wise load increase at the end of static SCC test in the tetra-thionic solution. As shown in Figure 9, we observed both the RD (Rapid drop) type corrosion and AE generation during the step increasing of AH. This strongly implies that new electrochemically active fresh surfaces are produced by mechanical breaking of the coincident grain. Amplitude of the corrosion drop reaches 8mV.

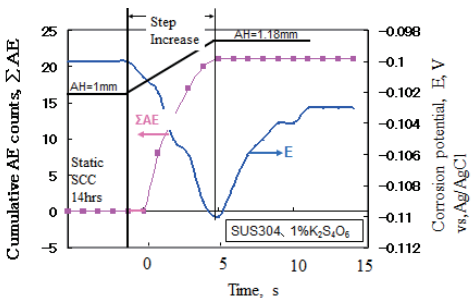


Figure 9: Change of AE and corrosion potential of the sensitized Type-304 steel during the static SCC test and step-wise load increase in the tetra-thionic solution

*3.2 IG-SCC of sensitized Type-316 by tetra-thionic acid*

Sensitized Type-316 strip (700 ℃ x 2 hours), as well the cold-rolled and then sensitized ones, show higher resistance against the tetra-thionic SCC than the Type-304 steel. However we observes the same AE behavior as those for the Type-304, ie., no AE during the static SCC test , but AEs of 30 to 60 counts during the crack opening operation. Here the authors show only the SEMs of the opened fracture surface. Figure 10 is SEM of the sensitized Type-316 of as-received strip and shows more star-fish type extrusions than the Type-304. Higher resistance of the Type-316 seems to be due to the frequent extrusions or the low energy boundaries. We can produce only one IG-SCC for the cold rolled (35%) and sensitized (700℃x2 hours) strips in pH=1.8 after 456 hours. We did not monitor AE during static SCC test but detected AEs during the crack opening operation. Figure 11 shows a number of extrusions in newly produced fracture surface, but no extrusion in the static SCC surface. The coincident grain boundary of the twins produced by cold working seems to be resistant to the IG-SCC.

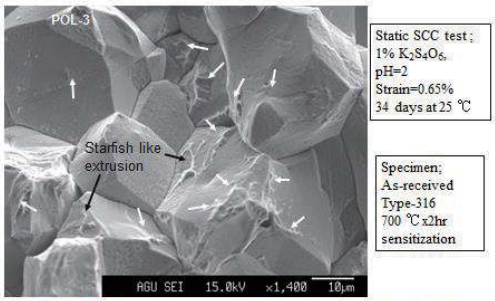


Figure 10: SEM of the fracture surface produced by crack opening operation in air of the sensitized type-316 steel previously suffered IG-SCC by static SCC test

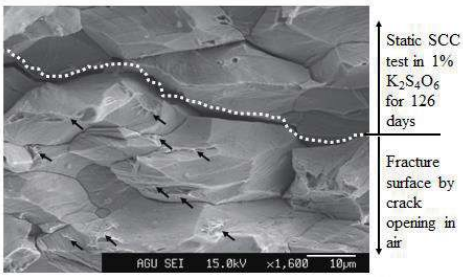


Figure 11: SEM of the fracture surface produced by crack opening operation in air of the 35% cold rolled and then sensitized (700 ℃x2 hrs) type-316 steel

*3.3 IG-SCC of as-received 70Cu/30Zn brass in ammonia vapor*

Among the brasses, 70%Cu/30%Zn brass shows IG-SCC in ammonia vapor from 2.5 mass % to 8 mass % at room temperature. We mainly studied IG-SCC of 70Cu/30 Zn brass in 8% ammonia vapor. Contrary the 60Cu/40Zn brass does not suffer TG-SCC and emit no AE during both the static SCC test and crack opening operation.

Figure 12 compares the crack length before and after the opening operation. The crack opening operation extends the SCC depth from 0.94 mm to 1.65 mm. Fractographic observation, Figure 13, revealed that the fracture surface by the static SCC is covered by thick corrosion products, but that by the opening operation is free from the products which makes detail SEM observation possible.

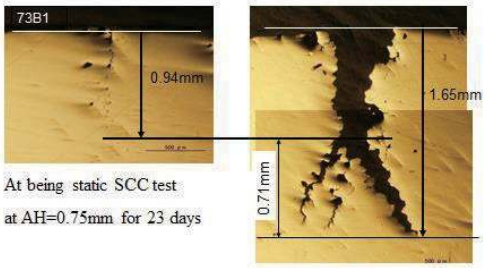


Figure 12: Transverse IG-SCC of 70/30 brass by 8% ammonia vapor.

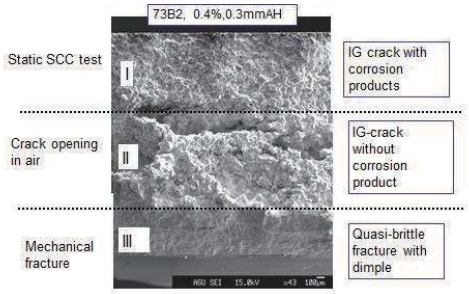


Figure 13:SEM of fracture surface of the brass attacked by 8% ammonia vapor and then crack opening operation in air

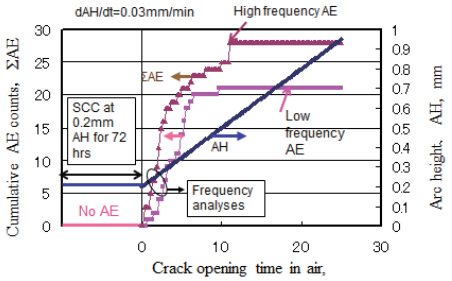


Figure 14 :Acoustic emission during static SCC test and crack opening in air of 70/30 brass previously attacked by 8% ammonia vapor

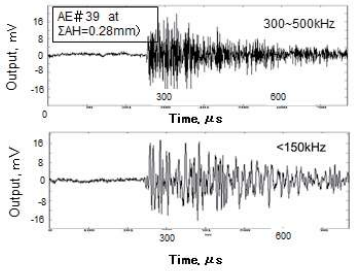


Figure15 : Waveform and frequency components spectrum of AE during crack opening operation of the 70/30 brass previously attacked by 8% ammonia

Figure 14 shows AE behavior during the static SCC test and crack opening operation. We also did not monitor AE during the static SCC test but monitored much AE signals during the crack opening. There fund to be two types of AEs, i.e., high frequency signals with frequency components from 300 to 500 kHz and low frequency component below 150 kHz, as shown in Figure15. Number of high frequency signals is slightly larger than those of low frequencies.

Examples of SEM of the new fracture surface are shown in both Figures 16 and 17. Figure 16 represents extrusions on the grains and open sub-crack around the grain with extrusions. Detail SEM observation revealed that there are another type of fracture as shown in Figure 17. We observe twin at the center of the photo, and quasi-cleavage fracture in the size of less than 25 $\mu$m. As the brass is much brittle than the austenitic stainless steel, this alloy is likely to suffer transgranular brittle fracture. This type of fracture is considered to correspond the mechanical cleavage fracture, suggested by the Film Induced Cracking (FIC)[9]. We did not observe the cleavage fracture started by brittle de-alloyed film during static loading, however, there is a possibility of the cleavage brittle fracture when we use dynamic strain increasing. We also monitored AE signals during the crack opening operation in ammonia vapor. It is not clear which signal with high frequency or low frequency is produced by which type of fracture shown in Figures 16 and 17.

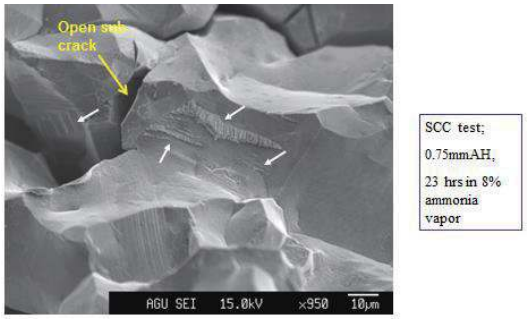


Figure 16 :SEM of the fracture surface produced by crack opening operation of the brass previously attacked by 8% ammonia vapor

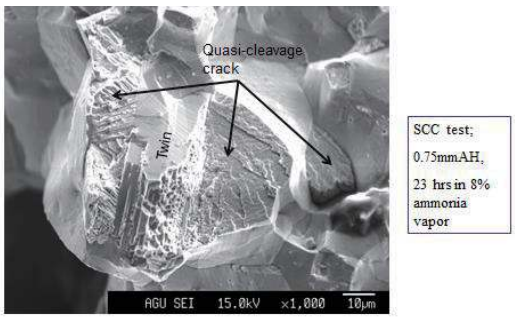


Figure 17: SEM of the fracture surface by crack opening operation of the brass previously attacked by 8% ammonia vapor

Figure 18 represents another example of brittle fracture which contains both the extrusion like projection and transgranular (TG) cleavage fracture. TG cleavage fracture suggests that the ammonia vapor impregnates into the cleavage plane and weakened the cohesion strength.

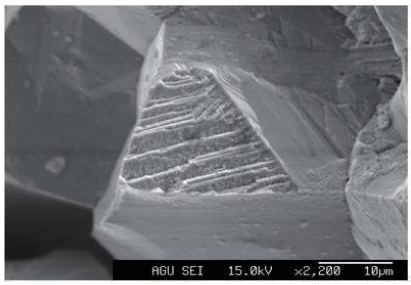


Figure 18 :SEM of the fracture surface by crack opening operation in air after the static SCC test

The AE behavior shown in Figure 14 is not limited to the ammonia SCC of the 70/30 brass. In the Mattson's solution

(pH=7.2, $NH_4OH+(NH_4)_2SO_4+CuSO_4$ soluti0on, recommended method by ASTM ), as shown in Figure 19, the 70Cu/30Zn brass emits no AE during the static SCC test but emits AEs during the crack opening operation.

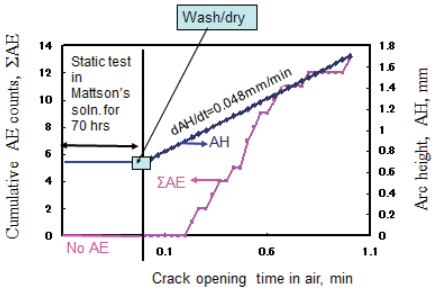


Figure 19: Acoustic emission during the static SCC test and crack opening in air of 70/30 brass previously attacked by Mattson's solution

## 5 CONCLUSIONS

Acoustic emission behavior is studied for the inter-granular SCC of sensitized Type-304 and -316 stainless steels in tetra-thionic acid and 70Cu/30Zn brass and ammonia vapor. Conclusions are summarized below:

1) We monitored no AE during static bending SCC test for both material/environment combinations, however monitored AEs during the crack opening operation (continuously load increasing or step wise load increasing) in air and in corrosive environment.
2) AEs from APC-SCC can be monitored only the dynamic loading to the IG-SCC. We can not monitor any primary AEs from transgranular type SCC.
3) Detail SEM observation suggests that the AEs during the crack opening operation are produced by mechanical fracture of the coincident grain boundary in case of both austenitic stainless steels and brass, and possibly by the quasi-cleavage trans granular fracture for the 70Cu/30Zn brass.
4) The intact grain boundary in our previous paper is considered to be the portion of low energy coincident grain boundary, such as the twin band/austenite grain boundary. The extrusion-like projections observed on the separated grain surfaces in non-corrosive environment appears to be the fracture trace of the coincident grain boundary.

## 5 REFERENCES

[1]Hideya Okada, Ken-ichi Yukawa and Hideo Tamura, Application of Acoustic Emission Technique to Study of Stress Corrosion Cracking in Distinguishing Between Active Path Corrosion and Hydrogen Embrittlement, Corrosion, 30-7(1974)pp. 253-255

[2]Kaita Ito, Hisashi Yamawaki, Hiroyuki Masuda, Mitsuharu Shiwa and Manabu Enoki, SCC Monitoring of Chloride Droplets on Thin SUS304 Plate Specimens by Analysis of Continuous Recorded AE Waveform, Materials Transaction, 51-8,(12010)pp.1409-1413

[3]M.Shiwa, H.Yamawaki, H.Matsuda, K.Ito and M.Enoki, Continuous And Burst AE Signal Analyses During Chloride Droplet SCC on Thin Plate of SUS304 Progress in Acoustic Emission XIV, 2008, pp.129-134

[4]M.Takemoto, H.Cho and K.Ono, Acoustic Emission during Stress Corrosion Cracking Tests, Duetsche Gesellshaft fur Zerstorungsfreie Prufung, 26th Europian Conference on Acoustic Emission Testing, (2004)pp. 617-629

[5] Mikio Takemoto, Motoaki Nakamura and Shuichi Ueno, Unique AE from Ammonia Stress Corrosion Cracking of Brass, Progress in Acoustic Emission XVI , (2012), pp139-144.

[6] Mikio Takemoto, Contribution of Acoustic Emission to Stress Corrosion Cracking Research, Advances in Acoustic Emission,(2007)pp.414-422

[7]M.Michiuchi, H.Kokawa, Z.J.Wang , Y.S.Sato and K.Sakai, Acta Materialia, 54, pp.5179-5184(2006)

[8]Hiroyuki Kokawa, Grain boundary Engineering, Application to Austenitic stainless steel II, Materia Japan, 52-2(2013)pp. 64-67

[9]K.Sieradzki and R.C.Newman, Brittle Behaviour of Ductile Metals During Stress Corrosion Cracking, Philosophical Magazine A,.51-1, (1985)pp.95-132